

# Design of Antenna–Sensitizer Polynuclear Complexes. Sensitization of Titanium Dioxide with [Ru(bpy)<sub>2</sub>(CN)<sub>2</sub>]<sub>2</sub>Ru(bpy(COO)<sub>2</sub>)<sub>2</sub><sup>2-</sup>

R. Amadelli, R. Argazzi, C. A. Bignozzi, and F. Scandola\*

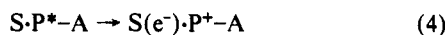
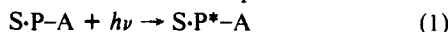
Contribution from the Dipartimento di Chimica dell'Università, Centro di Fotochimica C.N.R., 44100 Ferrara, Italy. Received January 30, 1990

**Abstract:** The use of antenna–sensitizer molecular devices is proposed as a possible strategy to increase the light harvesting efficiency of sensitized semiconductors. To illustrate this approach, the cyano-bridged trinuclear complex [Ru(bpy)<sub>2</sub>(CN)<sub>2</sub>]<sub>2</sub>Ru(bpy(COO)<sub>2</sub>)<sub>2</sub><sup>2-</sup> has been synthesized and studied. The complex adsorbs on TiO<sub>2</sub> via the negatively charged –Ru(bpy(COO)<sub>2</sub>)<sub>2</sub><sup>-</sup> central unit. The photophysical behavior in solution and the photoelectrochemical behavior on TiO<sub>2</sub> have been studied. Emission and excitation spectra show that in this complex the light energy absorbed by the terminal Ru(bpy)<sub>2</sub>(CN)<sub>2</sub> (antenna) groups is efficiently funneled to the central –Ru(bpy(COO)<sub>2</sub>)<sub>2</sub><sup>-</sup> (sensitizer) fragment. Photochemical spectra on TiO<sub>2</sub> demonstrate that the light absorbed by the antenna fragments is efficiently used for sensitization of the semiconductor.

## Introduction

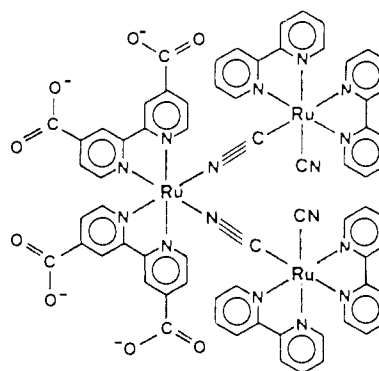
Dye sensitization, i.e., charge injection from an electronically excited adsorbed dye, is a well-established technique<sup>1,2</sup> that permits photoelectrochemical and photocatalytic processes on wide-bandgap semiconductors using sub-bandgap excitation. This feature is of obvious relevance to the use of semiconductors in solar energy conversion.<sup>3</sup> Recent examples of dye sensitization are those in which Ru(bpy(COO)<sub>2</sub>)<sub>3</sub><sup>4-</sup> (bpy(COO)<sub>2</sub><sup>2-</sup> = 4,4'-dicarboxy-2,2'-bipyridine) is used as a sensitizer on TiO<sub>2</sub>.<sup>4–6</sup> The main drawback of this technique is that, at a monolayer coverage, light absorption by the dye is often inefficient. On the other hand, multilayer adsorption does not help, as the inner layers tend to act as insulators with respect to the outer ones.<sup>7</sup> Thus, the only successful strategy to obtain good light harvesting efficiency of sensitized semiconductors has been so far that of increasing the surface area. In photocatalytic systems this can be achieved by using colloidal semiconductor particles.<sup>4,5</sup> In photoelectrochemical systems, substantial advances have been recently made with the use of electrodes of extremely high surface area, such as, e.g., the "fractal" TiO<sub>2</sub> electrodes developed by Graetzel.<sup>8</sup>

We would like to propose here a conceptually different (but likely complementary) strategy for improving the light absorption efficiency of a sensitized semiconductor. The idea is to substitute the sensitizer molecule at the semiconductor–solution interphase with a sensitizer–antenna molecular device.<sup>9–11</sup> Such a device is made of covalently linked "sensitizer" (P) and "antenna" (A) molecular fragments (components) and is adsorbed onto the semiconductor surface (S) through the sensitizer component. The function of the device is schematized in eq 1–4. The antenna



- (1) Gerischer, H.; Willig, F. *Top. Curr. Chem.* **1976**, *61*, 31.  
 (2) Memming, R. *Prog. Surface Sci.* **1984**, *17*, 7.  
 (3) Graetzel, M., Ed.; *Energy Resources Through Photochemistry and Catalysis*; Academic Press: New York, 1983.  
 (4) Desilvestro, J.; Graetzel, M.; Kavan, L.; Moser, J. *J. Am. Chem. Soc.* **1985**, *107*, 2988.  
 (5) Furlong, D. N.; Wells, D.; Sasse, W. H. F. *J. Phys. Chem.* **1986**, *90*, 1107.  
 (6) Vlachopoulos, N.; Liska, P.; Augustynski, J.; Graetzel, M. *J. Am. Chem. Soc.* **1988**, *110*, 1216.  
 (7) Gerischer, H. *Ber. Bunsenges. Phys. Chem.* **1973**, *77*, 771.  
 (8) Graetzel, M. In *Photochemical Energy Conversion*; Norris, J. R., Meisel, D., Eds.; Elsevier: New York, 1989.  
 (9) The machinery, architecture, functions, and possible applications of various light-driven ("photochemical") molecular devices have been recently discussed.<sup>10,11</sup>  
 (10) Balzani, V.; Moggi, L.; Scandola, F. In *Supramolecular Photochemistry*; Balzani, V., Ed.; Reidel: Dordrecht, 1987.  
 (11) Balzani, V.; Scandola, F. *Supramolecular Photochemistry*; Ellis Horwood: Chichester, 1990.

Scheme I



fragment has the role of absorbing strongly the incident light (eq 2) and transferring efficiently the electronic energy to the sensitizer fragment (eq 3), which then gives charge injection into the semiconductor (eq 4). In this way, both the light directly absorbed by the sensitizer (eq 1) and that absorbed by the antenna (eq 2) can be used to effect charge injection. With respect to a simple molecular sensitizer, such an antenna–sensitizer molecular device is expected to lead to an increase in the overall cross section for light absorption. How this increase is actually distributed over the action spectrum depends on the spectral characteristics of the antenna and sensitizer chromophores (subject to the obvious condition that  $h\nu' \geq h\nu$ ). In principle, antenna–sensitizer molecular devices with higher light harvesting efficiency could be designed making use of several antenna components in parallel (e.g., A–S–A) or in series (e.g., S–A–A), although for this last case efficient A-to-A energy transfer would be an additional requisite. This work represents a first attempt to put this idea at work.<sup>12</sup> It includes the design of a simple antenna–sensitizer molecular device and the test of its actual behavior on a semiconductor surface.

The design of the antenna–sensitizer device presented in this paper stems from our experience with photoinduced intramolecular processes in polynuclear metal complexes.<sup>13–18</sup> In the course of our previous work, we showed that in the trinuclear cyano-bridged complex [Ru(bpy)<sub>2</sub>(CN)<sub>2</sub>]<sub>2</sub>Ru(bpy)<sub>2</sub><sup>2+</sup> (bpy = 2,2'-bipyridine)

- (12) The use of antenna–sensitizer molecular devices in sensitization of semiconductors had previously been proposed on tentative grounds.<sup>13</sup>  
 (13) Bignozzi, C. A.; Chiorboli, C.; Indelli, M. T.; Rampi, M. A.; Scandola, F. *Coord. Chem. Rev.* **1990**, *97*, 299.  
 (14) Bignozzi, C. A.; Scandola, F. *Inorg. Chem.* **1984**, *23*, 1540.  
 (15) Bignozzi, C. A.; Roffia, S.; Scandola, F. *J. Am. Chem. Soc.* **1985**, *107*, 1644.  
 (16) Bignozzi, C. A.; Paradisi, C.; Roffia, S.; Scandola, F. *Inorg. Chem.* **1988**, *27*, 408.  
 (17) Bignozzi, C. A.; Indelli, M. T.; Scandola, F. *J. Am. Chem. Soc.* **1989**, *111*, 5192.  
 (18) Bignozzi, C. A.; Chiorboli, C.; Davila, J.; Indelli, M. T.; Scandola, F. *Inorg. Chem.* **1989**, *28*, 4350.

very efficient intramolecular energy transfer takes place from the peripheral  $\text{-Ru(bpy)}_2\text{-}$  chromophores (C bonded to both terminal and bridging cyanides) to the central  $\text{-Ru(bpy)}_2\text{-}$  chromophore (N-bonded to the bridging cyanides).<sup>18</sup> In other words, in this system the peripheral chromophores perform as efficient antenna components toward the central one. In other laboratories, it was shown that  $\text{Ru(bpy(COO)}_2)_3^{4-}$  is very effective in the sensitization of  $\text{TiO}_2$  in acidic solution.<sup>4-6</sup> In this sensitizer, the negatively charged carboxylate groups have the essential function of providing efficient adsorption of the complex onto the semiconductor (which in acidic solutions has a positively charged surface). Therefore, we thought that an antenna-sensitizer device for use on  $\text{TiO}_2$  could be derived from the basic structure of the above-mentioned trinuclear complex by addition of carboxylate groups to the bipyridines of the central unit, so as to provide to this unit the capability for adsorption on the semiconductor surface. The structure of the trinuclear complex  $[\text{Ru(bpy)}_2(\text{CN})_2]_2\text{Ru(bpy(COO)}_2)_2^{2-}$  is shown schematically in Scheme I. The present study reports on the synthesis and photophysical characterization of the complex and on its photoelectrochemical behavior on  $\text{TiO}_2$ .

### Experimental Section

**Materials.**  $(\text{NH}_4)_2\text{RuCl}_6$ , 2,2'-bipyridine-4,4'-dicarboxylic acid, and  $(\text{C}_2\text{H}_5)_4\text{NBF}_4$  ([TEA]TBF) were purchased from Aldrich.  $[\text{Ru(bpy)}_2(\text{CN})_2]_2\text{Ru(bpy)}_2^{2+}$  was available, as the hexafluorophosphate salt, from a previous study.<sup>18</sup> Acetonitrile for polarography (Carlo Erba) was used for the electrochemical measurements. All the other chemicals were of reagent grade.

**$\text{Ru(bpy(COOH)}_2)_2\text{C}_2\text{O}_4$ .**  $(\text{NH}_4)_2\text{RuCl}_6$  (1.04 g, 2.97 mmol) and  $\text{K}_2\text{C}_2\text{O}_4 \cdot \text{H}_2\text{O}$  (1.92 g, 10.4 mmol) were dissolved in 50 mL of water and heated for 2 h on a steam bath. Then, 1.25 g of 2,2'-bipyridine-4,4'-dicarboxylic acid (5.12 mmol) dissolved in 6 mL of 2 M NaOH was slowly added, and heating was continued for 2.5 h. The dark-brown solution was cooled to room temperature and concentrated to 15 mL, and a blue solid was filtered off. The solution was divided in three 5-mL portions that were separately chromatographed on Sephadex G15 columns ( $3 \times 70$  cm). Elution with 0.02 M NaCl gave a first blue fraction that was discarded, a second orange fraction of  $\text{Ru(bpy(COO)}_2)_3^{4-}$  (that is an interesting byproduct of this synthesis), and a third deep-violet fraction of  $\text{Ru(bpy(COO)}_2)_2\text{C}_2\text{O}_4^{4-}$ . The violet fractions from the three chromatographic separations were put together and concentrated to 20 mL; 0.25 M HCl was added dropwise until complete precipitation of the uncharged product. The violet solid was washed with water and vacuum dried. Anal. Calcd for  $\text{Ru(bpy(COOH)}_2)_2\text{C}_2\text{O}_4 \cdot 2\text{H}_2\text{O}$ : C, 43.77; N, 7.85; H, 2.82. Found: C, 43.29; N, 7.87; H, 2.90. The sodium salt was obtained by dissolving the complex in an aqueous solution containing an equivalent amount of NaOH, followed by evaporation and vacuum drying. The tetraethylammonium salt was obtained from the sodium salt by ion exchange chromatography. The infrared spectrum of the  $\text{Ru(bpy(COO)}_2)_2\text{C}_2\text{O}_4^{4-}$  is an almost exact superposition of those of  $\text{Ru(bpy(COO)}_2)_3^{4-}$  (obtained as a byproduct; vide supra) and  $\text{Ru(bpy)}_2\text{C}_2\text{O}_4^{19}$ .

**$[\text{Ru(bpy)}_2(\text{CN})_2]_2\text{Ru(bpy(COO)}_2)_2$ .**  $\text{Na}_4[\text{Ru(bpy(COO)}_2)_2\text{C}_2\text{O}_4]$  (0.15 g, 0.2 mmol) was dissolved in 10 mL of water and slowly added to a 70-mL  $\text{CH}_3\text{OH}$  solution containing 1.0 g of  $\text{Ru(bpy)}_2(\text{CN})_2 \cdot 2\text{H}_2\text{O}$  (2.0 mmol). To the solution was added 1 mL of 2 M HCl and the mixture was refluxed for 20 h. The solution was concentrated to 10 mL and cooled to room temperature; 1 mL of 2 M NaOH was added. Orange crystals of  $\text{Ru(bpy)}_2(\text{CN})_2$  were filtered off. The solution was further concentrated to 5 mL and loaded on a  $3 \times 70$  cm Sephadex G15 column. The first brown fraction eluted was collected, leaving on the column a yellow fraction made of  $\text{Ru(bpy)}_2(\text{CN})_2$ . The brown fraction was loaded on a Sephadex DEAE-A25 anion-exchange column. The brown trinuclear complex was eluted with 0.05 M NaOH, leaving a small amount of the violet unreacted  $\text{Ru(bpy(COO)}_2)_2\text{C}_2\text{O}_4^{4-}$  in the column. The brown fraction was concentrated to 10 mL, and 2 M HCl was added dropwise until complete precipitation of the neutral form. The solid was washed with water and dried under vacuum. Anal. Calcd for  $[\text{Ru(bpy)}_2(\text{CN})_2]_2\text{Ru(bpy(COO)}_2)_2 \cdot 6\text{H}_2\text{O}$ : C, 50.40; N, 13.84; H, 3.50. Found: C, 50.49; N, 14.02; H, 3.36.

**$\text{Na}_2[\text{Ru(bpy)}_2(\text{CN})_2]_2\text{Ru(bpy(COO)}_2)_2$**  was obtained by dissolution of  $[\text{Ru(bpy)}_2(\text{CN})_2]_2\text{Ru(bpy(COO)}_2)_2$  in a stoichiometric amount of aqueous NaOH followed by evaporation and vacuum drying.  **$(t\text{-Bu}_4\text{N})_2[\text{Ru(bpy)}_2(\text{CN})_2]_2\text{Ru(bpy(COO)}_2)_2$**  was obtained from the sodium salt by ion-exchange chromatography followed by evaporation

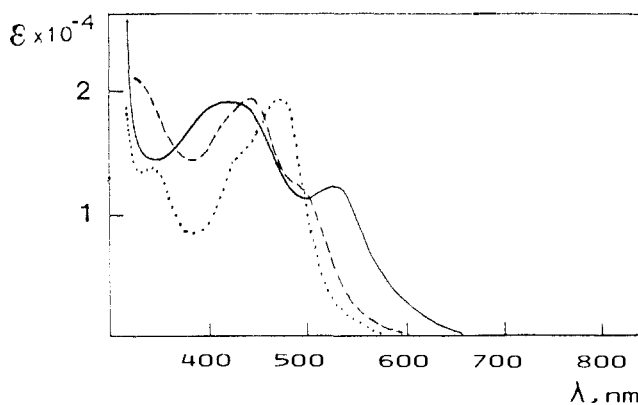


Figure 1. Absorption spectra of  $[\text{Ru(bpy)}_2(\text{CN})_2]_2\text{Ru(bpy(COO)}_2)_2^{2-}$  (full line),  $[\text{Ru(bpy)}_2(\text{CN})_2]_2\text{Ru(bpy)}_2^{2+}$  (dashed line), and  $\text{Ru(bpy(COO)}_2)_3^{4-}$  (dotted line) in aqueous (pH 3.5) solution.

and vacuum drying. The infrared spectrum of the  $[\text{Ru(bpy)}_2(\text{CN})_2]_2\text{Ru(bpy(COO)}_2)_2^{2-}$  ion (in this or in the sodium salt) is an almost exact superposition of those of  $[\text{Ru(bpy)}_2(\text{CN})_2]_2\text{Ru(bpy)}_2^{2+}$  and  $\text{Ru(bpy(COO)}_2)_3^{4-}$  (obtained as a byproduct in the previous preparation; vide supra).

**Apparatus and Procedures.** UV-vis spectra were recorded with a Perkin-Elmer 323 spectrophotometer. Infrared spectra were obtained with a Bruker IFS88 FTIR instrument. Emission and excitation spectra were taken on a Perkin-Elmer MPF 44E spectrofluorimeter equipped with a Hamamatsu R928 tube. The emission spectra were corrected for instrumental response by calibration with a NBS standard quartz-halogen lamp.

Emission lifetimes were determined with a PRA 3000 nanosecond fluorescence spectrometer equipped with a Model 510B nanosecond pulsed lamp and a Model 1551 cooled photomultiplier; the data were collected on a Tracor Northern multichannel analyzer and processed on a PDP11/03 computer using original PRA software.

Cyclic voltammetric (CV) measurements were carried out in  $\text{CH}_3\text{CN}$  with an AMEL 552 potentiostat and an AMEL 568 programmable function generator, with the output plotted on an AMEL 863 X/Y recorder. Minimization of uncompensated resistance was achieved with a positive feedback network of the potentiostat. Potential sweep voltammetric curves at potential sweep rates higher than 300 mV/s were recorded by means of the AMEL 448 three-electrode oscillographic polarograph. A saturated calomel electrode was used as reference electrode. A glassy carbon electrode and a stationary platinum electrode were used as working electrodes. The cell configuration was such that it was possible to perform experiments with the working and counter electrode compartment at low temperature, while the reference electrode was kept at room temperature. The supporting electrolyte was 0.1 M [TEA]TBF. Values of  $E_{1/2}$  were calculated by averaging the oxidative and reductive peak potentials.

The photoelectrochemical experiments were carried out using as photoelectrode a 1-cm<sup>2</sup> titanium sheet onto which a  $\text{TiO}_2$  layer (ca. 3  $\mu\text{m}$ ) was deposited by painting titanium isopropoxide in 2-propanol, followed by hydrolysis and heating at 500 °C. Adsorption of the sensitizer was obtained by immersion (20 min) of the photoelectrode in a  $1 \times 10^{-4}$  M solution of the sensitizer at pH 3.5 ( $\text{H}_2\text{SO}_4$ ) followed by rinsing. Photocurrents were measured with an AMEL equipment in a conventional three-compartment cell, at a potential corresponding to the photocurrent plateau value (+0.1 V versus SCE). The electron donor was NaI (0.1 M). Illumination was performed with a 250-W Xe lamp/monochromator combination. Light intensity values (in the  $\text{mW cm}^{-2}$  range) were measured with an IL 700 Research radiometer. Photocurrent efficiencies were calculated using standard equations.<sup>6</sup>

Adsorption of trinuclear and mononuclear complexes on  $\text{TiO}_2$  powders (Degussa P25) was performed by stirring (1 h) a suspension of the powder (2 mg/mL) in  $1-2 \times 10^{-4}$  M solutions of the complex at pH 3.5 ( $\text{H}_2\text{SO}_4$ ). The amount of complex adsorbed was determined spectrophotometrically from the complex concentration left in solution after centrifugation.

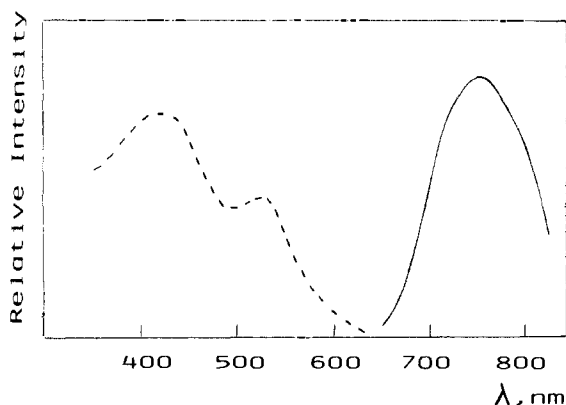
### Results

Aqueous solutions of the complex (pH 2–10) were stable for periods of weeks. The absorption spectrum of  $[\text{Ru(bpy)}_2(\text{CN})_2]_2\text{Ru(bpy(COO)}_2)_2$  (sodium salt) in aqueous solutions at pH 3.5 is shown, together with those of two related species (the mononuclear carboxylate complex  $\text{Ru(bpy(COO)}_2)_3^{4-}$  and the trinuclear noncarboxylated complex  $[\text{Ru(bpy)}_2(\text{CN})_2]_2\text{Ru}$

**Table I.** Redox Properties of  $[\text{Ru}(\text{bpy})_2(\text{CN})_2]_2\text{Ru}(\text{bpy}(\text{COO})_2)_2^{2-}$  and Its Parent Unsubstituted Species<sup>a</sup>

complex	$E_{1/2}^{\text{ox}}$			$E_{1/2}^{\text{red}}$		ref
	(1)	(2)	(3)	(1)	(2)	
$[\text{Ru}(\text{bpy})_2(\text{CN})_2]_2\text{Ru}(\text{bpy}(\text{COO})_2)_2^{2-}$	+0.54	+1.24 <sup>b</sup>	+1.58 <sup>b,c</sup>	-1.61 <sup>d</sup>	-1.74	<i>e</i>
$[\text{Ru}(\text{bpy})_2(\text{CN})_2]_2\text{Ru}(\text{bpy})_2^{2+}$	+0.66 <sup>f</sup>	+1.19 <sup>f</sup>	+1.46 <sup>f</sup>	-1.54 <sup>d</sup>	-1.65	18, <i>e</i>

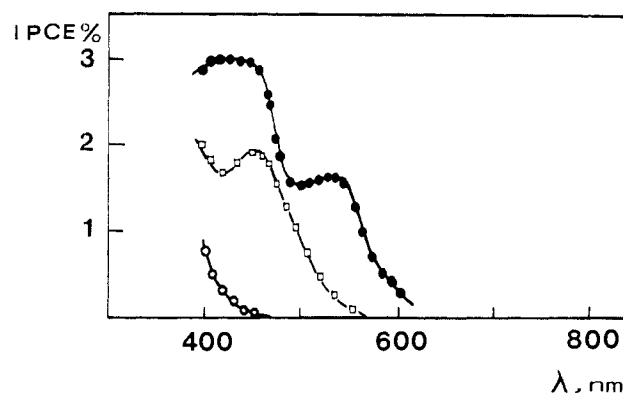
<sup>a</sup> Voltammetric potentials (versus SCE) in acetonitrile at  $-30^\circ\text{C}$ ; scan rate 0.2 V/s, unless otherwise noted. <sup>b</sup> Scan rate, 1.5 V/s. <sup>c</sup> Irreversible voltammetric wave, anodic peak potential. <sup>d</sup> The intensity of this voltammetric wave is approximately twice that of  $E_{1/2}^{\text{ox}}(1)$  and  $E_{1/2}^{\text{red}}(2)$ . <sup>e</sup> This work. <sup>f</sup> Room-temperature data.

**Figure 2.** Emission (full line) and excitation (dashed line) spectra of  $[\text{Ru}(\text{bpy})_2(\text{CN})_2]_2\text{Ru}(\text{bpy}(\text{COO})_2)_2^{2-}$  in aqueous (pH 3.5) solution.

$(\text{bpy})_2^{2+})^{18}$  in Figure 1. The spectrum of  $[\text{Ru}(\text{bpy})_2(\text{CN})_2]_2\text{Ru}(\text{bpy}(\text{COO})_2)_2^{2-}$  at pH 3.5 is practically identical with those recorded in neutral or alkaline solutions, indicating that at this pH the carboxylate groups are still essentially unprotonated. By increasing the acidity of the solution to the limit (pH ca. 2.0) where precipitation of the diprotonated neutral form of the complex begins, the low-energy band undergoes a red shift ( $\lambda_{\text{max}} = 526$  and 540 nm at pH 3.5 and 2.0, respectively) while the position of the high-energy band does not appreciably change.<sup>20</sup>

Cyclic voltammetry of  $[\text{Ru}(\text{bpy})_2(\text{CN})_2]_2\text{Ru}(\text{bpy}(\text{COO})_2)_2^{2-}$  (tetrabutylammonium salt) in acetonitrile at room temperature in the range 0.0–1.0 V gave rise to a reversible wave with  $E_{1/2}^{\text{ox}}(1) = +0.54$  V (versus SCE). In the range 1.0–1.7 V, two irreversible waves were observed. Upon cooling to  $-30^\circ\text{C}$  and at high scan rates (1.5 V/s) the first of these waves became reversible with  $E_{1/2}^{\text{ox}}(2) = +1.24$  V, while the second one remained irreversible with anodic peak potential +1.58 V. In the range 0.0–(-1.9) V, two appreciably reversible waves were observed with  $E_{1/2}^{\text{red}}(1) = -1.61$  and  $E_{1/2}^{\text{red}}(2) = -1.74$  V (separation of cathodic and anodic peaks, 70 and 60 mV, respectively). Based on its intensity, which is approximately twice those corresponding to the second reduction and first oxidation processes, the first reduction wave appears to consist of two closely lying one-electron processes. The electrochemical data are summarized in Table I, where the corresponding data for the related  $[\text{Ru}(\text{bpy})_2(\text{CN})_2]_2\text{Ru}(\text{bpy})_2^{2+}$  complex<sup>18</sup> are also given for comparison (the  $E_{1/2}^{\text{red}}$  data for this complex, which were not available from previous work,<sup>18</sup> have been measured in analogous cyclic voltammetric experiments). Aqueous (pH 3.5) solutions of the one-electron oxidized product  $[\text{Ru}(\text{bpy})_2(\text{CN})_2]_2\text{Ru}(\text{bpy}(\text{COO})_2)_2^-$ , obtained by electrochemical oxidation of  $[\text{Ru}(\text{bpy})_2(\text{CN})_2]_2\text{Ru}(\text{bpy}(\text{COO})_2)_2^{2-}$  at +0.9 V (versus SCE) or by chemical oxidation with  $\text{Br}_2$ , are stable over a period of several hours.

Aqueous solutions of  $[\text{Ru}(\text{bpy})_2(\text{CN})_2]_2\text{Ru}(\text{bpy}(\text{COO})_2)_2^{2-}$  are appreciably photostable upon irradiation with visible light. The complex emits in room-temperature aqueous solution. The emission spectrum at pH 3.5 is shown in Figure 2. The emission ( $\lambda_{\text{max}} 760$  nm) decays as a single exponential with lifetime of 19 ns. The excitation spectrum of this emission is also shown in Figure 2. The emission does not apparently shift but undergoes

**Figure 3.** Photocurrent spectra of a  $\text{TiO}_2$  electrode coated with:  $[\text{Ru}(\text{bpy})_2(\text{CN})_2]_2\text{Ru}(\text{bpy}(\text{COO})_2)_2^{2-}$  (full circles),  $\text{Ru}(\text{bpy}(\text{COO})_2)_3^{4-}$  (squares), no sensitizer (circles). Aqueous 0.1 M NaI (pH 3.5).

a substantial increase in intensity and lifetime ( $\tau$  29 ns) when the pH of the solution is increased to  $\text{pH} \geq 5$ .<sup>20</sup>

In aqueous solution at pH 3.5,  $[\text{Ru}(\text{bpy})_2(\text{CN})_2]_2\text{Ru}(\text{bpy}(\text{COO})_2)_2^{2-}$  adsorbs efficiently on  $\text{TiO}_2$  powders (Degussa P25) giving a purple color to the solid. Comparative adsorption measurements under saturation conditions (see Experimental Section) indicated that at this pH the adsorption of the trinuclear complex is comparable to that of the mononuclear  $\text{Ru}(\text{bpy}(\text{COO})_2)_3^{4-}$  complex ( $2.5 \times 10^{-5}$  and  $1.9 \times 10^{-5}$  mol/g, respectively). In the same experimental conditions, neither  $\text{Ru}(\text{bpy})_2(\text{CN})_2$  nor the trinuclear analogue lacking the carboxylate substituents,  $[\text{Ru}(\text{bpy})_2(\text{CN})_2]_2\text{Ru}(\text{bpy})_2^{2+}$ , undergoes any appreciable adsorption. The adsorption of the complexes onto the  $\text{TiO}_2$  electrodes used in the photoelectrochemical experiments (vide infra) could not be measured by similar experiments, because of the low surface area of the electrodes and the consequently small fractional concentration changes occurring in solution.

Photoelectrochemical experiments were performed using a  $\text{TiO}_2$ -coated electrode and NaI as electron donor in aqueous pH 3.5 solution (see Experimental Section). The photocurrent spectrum obtained with the bare electrode is shown in Figure 3. Adsorption of  $[\text{Ru}(\text{bpy})_2(\text{CN})_2]_2\text{Ru}(\text{bpy}(\text{COO})_2)_2^{2-}$  on the electrode was performed by immersion (20 min) of the electrode in a  $1 \times 10^{-4}$  M solution of the complex followed by rinsing with water. The photocurrent spectrum obtained with such a loaded electrode is shown in Figure 3. For purposes of comparison, the photocurrent spectrum obtained by loading the same electrode with the mononuclear  $\text{Ru}(\text{bpy}(\text{COO})_2)_3^{4-}$  complex under comparable conditions is also shown in Figure 3. On the vertical scale, the comparison between the three spectra of Figure 3 is to be taken as an approximate one, since the reproducibility of the photocurrent efficiencies obtained in repeated experiments (made by reloading the same dye onto the photoelectrode after desorption in alkaline solution) was relatively poor (not better than  $\pm 30\%$ ).

## Discussion

The  $[\text{Ru}(\text{bpy})_2(\text{CN})_2]_2\text{Ru}(\text{bpy}(\text{COO})_2)_2^{2-}$  complex has been synthesized in an attempt to demonstrate the use of antenna-sensitizer molecular devices in the sensitization of semiconductors. In the design of such a trinuclear complex, the following objectives were pursued: (i) the complex should feature an antenna effect, with light energy absorbed by the peripheral units being efficiently transferred to the central unit; (ii) the complex should bind to the semiconductor surface via the central unit; (iii) following

(20) A more detailed account of the ground- and excited-state proton transfer behavior of this complex will be given elsewhere: Bignozzi, C. A.; Scandola, F., manuscript in preparation.

excitation (both by direct light absorption and by energy transfer from the peripheral units), the central unit of the complex should perform electron injection into the semiconductor. In this discussion, the performance of  $[\text{Ru}(\text{bpy})_2(\text{CN})_2]_2\text{Ru}(\text{bpy}(\text{COO})_2)_2^{2-}$  with respect to these objectives will be examined.

**Energy Levels and Photophysical Behavior.** In Ru(II)-polypyridine complexes, useful information about the energy of metal-to-ligand charge-transfer (MLCT) excited states can often be obtained from electrochemical data, since the metal and ligand orbitals involved in the spectroscopic transition are the same involved in oxidation and reduction, respectively.<sup>21</sup> In particular, in polynuclear complexes the relative energy ordering of MLCT states belonging to different subunits can be established if the electrochemical potentials can be unambiguously assigned to the various redox centers.<sup>18,22-24</sup>

In previous work with the parent  $[\text{Ru}(\text{bpy})_2(\text{CN})_2]_2\text{Ru}(\text{bpy})_2^{2+}$  complex,<sup>18</sup> it was shown that the oxidation of the central ruthenium ( $E_{1/2}^{\text{ox}}(1)$  in Table I) is much easier than that of the terminal ones ( $E_{1/2}^{\text{ox}}(2)$  and  $E_{1/2}^{\text{ox}}(3)$ )<sup>25</sup> due to the poor  $\pi$ -acceptor (ammonia-like) character of the N-bonded cyanides of this unit. As to the reduction processes, which involve the bipyridine ligands of the various units, the one-electron process  $E_{1/2}^{\text{red}}(2)$  (Table I) is assigned to the central unit and the two-electron process  $E_{1/2}^{\text{red}}(1)$  (Table I) to the peripheral units. Following the general correlation of MLCT energies with  $E^{\text{ox}} - E^{\text{red}}$ ,<sup>21</sup> in  $[\text{Ru}(\text{bpy})_2(\text{CN})_2]_2\text{Ru}(\text{bpy})_2^{2+}$ , the chromophore with the lowest MLCT excited states (both of singlet and triplet multiplicity) is the central, N-bonded  $-\text{Ru}(\text{bpy})_2-$  unit.<sup>18</sup>

The spectroscopic assignments for the  $[\text{Ru}(\text{bpy})_2(\text{CN})_2]_2\text{Ru}(\text{bpy}(\text{COO})_2)_2^{2-}$  complex follow closely those of the parent complex. In fact, it is seen in Table I that the presence of carboxylate groups on the bipyridines of the central unit produces a cathodic shift in the potentials for both oxidation and reduction of the central unit ( $E_{1/2}^{\text{ox}}(1)$  and  $E_{1/2}^{\text{red}}(2)$ ). Since the shift is somewhat larger for oxidation than for reduction (leading to a slight decrease in  $E_{1/2}^{\text{ox}}(1) - E_{1/2}^{\text{red}}(2)$ ), carboxyl substitution does not change the relative energy ordering of the MLCT states localized on the central and peripheral units. Thus, the singlet MLCT state of the central  $-\text{Ru}(\text{bpy}(\text{COO})_2)_2-$  unit is responsible for the lowest energy transition in the absorption spectrum. This transition, which in the parent complex only showed up as a shoulder in the low-energy part of the visible spectrum, appears here as an individual band ( $\lambda_{\text{max}}$  526 nm), well-resolved from the MLCT band of the peripheral units (Figure 1). The ratio between the intensities of the two bands clearly supports the assignment. Also, the behavior observed for the two bands (red shift of the low-energy band, no shift for the high-energy one) upon protonation of the carboxylate groups<sup>20,26,27</sup> labels the low-energy band as belonging to the central chromophore.

The arguments used for assigning the relative energy ordering of the singlet MLCT states of  $[\text{Ru}(\text{bpy})_2(\text{CN})_2]_2\text{Ru}(\text{bpy}(\text{COO})_2)_2^{2-}$  can be extended to the triplets, leading to the qualitative energy level diagram shown in Figure 4. In this complex, emission by the terminal chromophores is expected to occur at ca. 600 nm, taking the  $[\text{Ru}(\text{bpy})_2(\text{CN})_2]\text{Pt}(\text{dien})^{2+}$  complex ( $\lambda_{\text{max}}^{\text{abs}}$  416 nm,  $\lambda_{\text{max}}^{\text{em}}$  590 nm)<sup>14</sup> as a reasonable model for singly metalated  $\text{Ru}(\text{bpy})_2(\text{CN})_2$ . That from the central chromophore, based on the absorption-emission shift of the parent  $[\text{Ru}(\text{bpy})_2(\text{CN})_2]_2\text{Ru}(\text{bpy})_2^{2+}$  complex (ca. 0.6  $\mu\text{m}^{-1}$  in  $\text{H}_2\text{O}$ ),<sup>18</sup> is expected at ca. 770 nm. The results show that  $[\text{Ru}(\text{bpy})_2(\text{CN})_2]_2\text{Ru}(\text{bpy}(\text{COO})_2)_2^{2-}$  gives rise to a single emission band at 760 nm (Figure 2). The emission undergoes a single-exponential decay and has an excitation spectrum (Figure 2) that coincides with the absorption spectrum (Figure 1). These facts clearly indicate that emission occurs from the central chromophore and that very efficient intramolecular energy transfer from the MLCT states of the peripheral units to the triplet state of the central chromophore occurs in this system (Figure 4).<sup>28,29</sup> The localization of the emission on the chromophore containing the carboxylate groups is also demonstrated by the pH dependence of the emission lifetime.<sup>20,27,30-32</sup> The lack of any measurable risetime in single-photon counting experiments and the complete absence of emission from the peripheral units indicate that the rate constant for intramolecular energy transfer in this system is  $\geq 10^9 \text{ s}^{-1}$ .

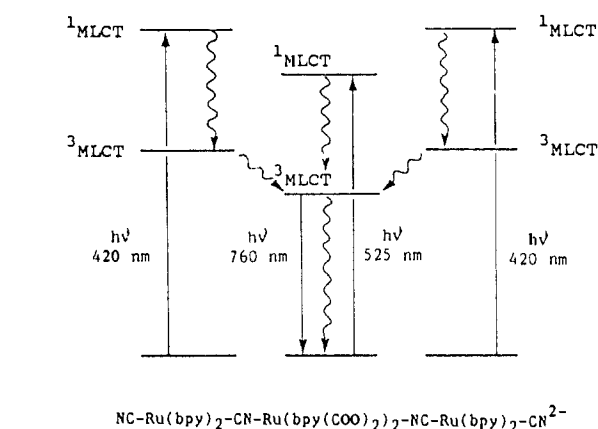


**Figure 4.** Qualitative energy level diagram and mechanism of the antenna effect in  $[\text{Ru}(\text{bpy})_2(\text{CN})_2]_2\text{Ru}(\text{bpy}(\text{COO})_2)_2^{2-}$ .

that in  $[\text{Ru}(\text{bpy})_2(\text{CN})_2]_2\text{Ru}(\text{bpy}(\text{COO})_2)_2^{2-}$  the two terminal  $-\text{Ru}(\text{bpy})_2-$  units act as efficient antenna groups with respect to the central  $-\text{Ru}(\text{bpy}(\text{COO})_2)_2-$  fragment.

**Adsorption on  $\text{TiO}_2$ .** The mononuclear sensitizer  $\text{Ru}(\text{bpy}(\text{COO})_2)_3^{4-}$  is known to adsorb efficiently on  $\text{TiO}_2$  powders, colloids, and electrodes in the 3–6 pH range.<sup>4-6</sup> This adsorption is the result of electrostatic attraction between the sensitizer, which in this pH range is anionic, and the semiconductor particle, which in this pH range is positively charged (isoelectric point of  $\text{TiO}_2$ , ca. pH 6). The adsorption can be easily reversed in alkaline solution.<sup>4-6</sup>

The results obtained with  $[\text{Ru}(\text{bpy})_2(\text{CN})_2]_2\text{Ru}(\text{bpy}(\text{COO})_2)_2^{2-}$  are qualitatively similar to those with  $\text{Ru}(\text{bpy}(\text{COO})_2)_3^{4-}$ , as far as the pH range of absorption and desorption is concerned. The quantitative comparison also shows that the two complexes adsorb on  $\text{TiO}_2$  powders in comparable amounts. Therefore, the re-

(28) In principle, the energy-transfer steps could occur in this system either at the singlet (Coulombic energy transfer)<sup>28</sup> or at the triplet (exchange energy transfer)<sup>29</sup> level. No experimental discrimination between the two mechanisms is possible. Given (i) the very short lifetime of singlet MLCT states in Ru(II) polypyridine complexes<sup>21</sup> and (ii) the ability of bridging cyanide to propagate electronic interaction between metal centers,<sup>15,16,18</sup> a triplet pathway with exchange energy transfer is considered more likely in this system.

(29) Turro, N. J. *Modern Molecular Photochemistry*, Benjamin: Menlo Park, CA, 1978.

(30) The fact that changes in emission and absorption take place in different pH ranges (2.0–3.5 and 3.0–5.0, respectively) is in keeping with the expectation that the carboxylic groups are less acidic in the MLCT excited state than in the ground state.

(31) The emission strongly decreases in intensity and lifetime by changing the pH from 5.0 to 3.5, as a consequence of substantial excited-state protonation of the carboxylate groups. The expected<sup>27</sup> red shift, on the other hand, cannot be easily observed because of the weakness of the emission of the protonated form relative to the residual emission of the unprotonated one (a shift to ca. 820 nm can actually be observed when such residual emission is completely eliminated by going at pH 2).<sup>20</sup> The decrease in lifetime upon protonation is easily understandable as a consequence of the lowering in energy of the MLCT state, based on energy-gap-law arguments.<sup>32</sup>

(32) Meyer, T. J. *Pure Appl. Chem.* **1986**, *58*, 1193.

(21) Juris, A.; Balzani, V.; Barigelletti, F.; Campagna, S.; Belser, P.; von Zelewski, A. *Coord. Chem. Rev.* **1988**, *84*, 85.

(22) Sahai, R.; Morgan, L.; Rillema, D. P. *Inorg. Chem.* **1988**, *27*, 3495.

(23) Murphy, W. R.; Brewer, K. J.; Gettiffe, G.; Petersen, J. D. *Inorg. Chem.* **1989**, *28*, 81.

(24) Campagna, S.; Denti, G. F.; Sabatini, L.; Serroni, S.; Ciano, M.; Balzani, V. *J. Chem. Soc., Chem. Commun.* **1989**, 1500.

(25) The potentials for oxidation of the two terminal units exhibit a relatively high separation, indicating a relatively high degree of electronic coupling between the metal centers through the bridging cyanide chain.<sup>18</sup>

(26) In addition to the carboxylate groups, the trinuclear complex also has two nonbridging cyanides as potential sites for protonation. Protonation of the cyanides, however, occurs in a much lower pH range (pH  $\leq 1$ ).<sup>20</sup>

(27) A decrease in the energy of the MLCT states is expected on the basis of the increase in electron acceptor character of the carboxylic groups upon protonation.

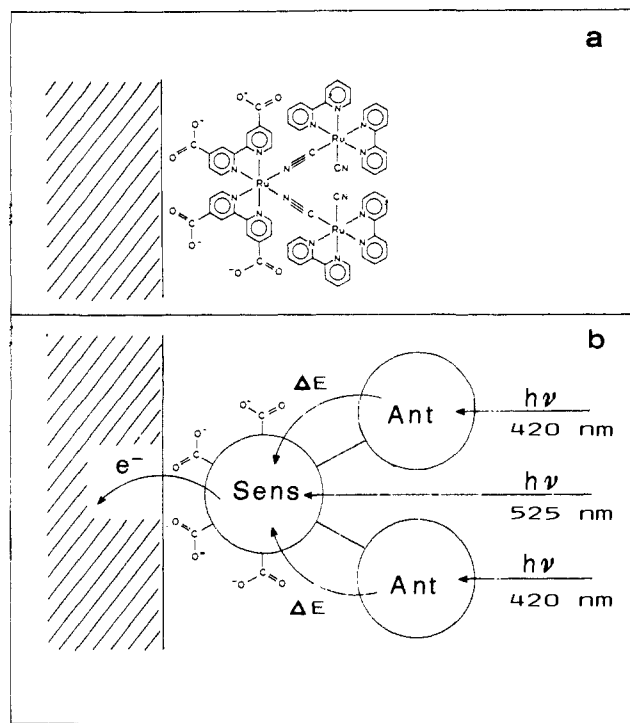


**Figure 5.** (a) Schematic representation of the mode of adsorption of the trinuclear complex on the TiO<sub>2</sub> surface. (b) Block diagram showing the function of the trinuclear complex as an antenna-sensitizer molecular device.

placement of one  $\text{bpy}(\text{COO})_2^-$  ligand of the mononuclear complex with the two terminal  $\text{Ru}(\text{bpy})_2(\text{CN})_2$  chromophores is not prejudicial to efficient adsorption. This suggests that in both cases the interaction of the  $-\text{Ru}(\text{bpy}(\text{COO})_2)_2^-$  unit with the surface is the relevant point, while the changes in overall (negative) charge brought about by the rest of the molecule play a relatively minor role.

On the other hand, both the noncarboxylated analogue  $[\text{Ru}(\text{bpy})_2(\text{CN})_2]_2\text{Ru}(\text{bpy})_2^{2+}$  and  $\text{Ru}(\text{bpy})_2(\text{CN})_2$  do not adsorb to any appreciable extent on TiO<sub>2</sub> in this pH range. These compounds have been used to test the possibility that the peripheral units of  $[\text{Ru}(\text{bpy})_2(\text{CN})_2]_2\text{Ru}(\text{bpy}(\text{COO})_2)_2^{2-}$  might have some nonelectrostatic affinity (e.g., via the free cyanides) for interaction with the surface of the semiconductor. The lack of adsorption of these model compounds indicates that no such affinity is present and suggests that in the adsorbed  $[\text{Ru}(\text{bpy})_2(\text{CN})_2]_2\text{Ru}(\text{bpy}(\text{COO})_2)_2^{2-}$  the positively charged<sup>33</sup> peripheral units most probably avoid the TiO<sub>2</sub> surface.

In conclusion, the  $[\text{Ru}(\text{bpy})_2(\text{CN})_2]_2\text{Ru}(\text{bpy}(\text{COO})_2)_2^{2-}$  trinuclear complex is bound to the TiO<sub>2</sub> surface via electrostatic interactions at the carboxylate groups of the central unit and is probably oriented as shown in Figure 5a.

**Photoelectrochemical Behavior.** The photocurrents observed on TiO<sub>2</sub> electrodes coated with  $[\text{Ru}(\text{bpy})_2(\text{CN})_2]_2\text{Ru}(\text{bpy}(\text{COO})_2)_2^{2-}$  indicate that photoelectron injection occurs in the system. In Figure 3, the photocurrent spectrum obtained on the same electrode with  $\text{Ru}(\text{bpy}(\text{COO})_2)_3^{4-}$  is shown for comparison. Based on the experiments with TiO<sub>2</sub> powders, the mononuclear and the trinuclear complex are expected to adsorb at the electrode in comparable amounts. Within the limits of reproducibility of repeated photoelectrochemical experiments noticed in the Results section, the photocurrent intensities obtained upon excitation in

(33) It is difficult to assign integral electric charges to the various chromophoric units in the polynuclear complex. The charge of each terminal unit is either 0 or +1, depending on which unit the bridging cyanides are assigned to.

the lowest absorption band of the two complexes (Figure 3) indicate that the efficiency of electron injection of  $[\text{Ru}(\text{bpy})_2(\text{CN})_2]_2\text{Ru}(\text{bpy}(\text{COO})_2)_2^{2-}$  is at least as good as that (60%<sup>4</sup> or more<sup>6</sup>) of its mononuclear analogue.

The photocurrent spectrum obtained with  $[\text{Ru}(\text{bpy})_2(\text{CN})_2]_2\text{Ru}(\text{bpy}(\text{COO})_2)_2^{2-}$  (Figure 3) is a demonstration of the operation of the antenna effect in the TiO<sub>2</sub> sensitization process. In fact, the photocurrent spectrum reproduces closely the absorption spectrum of the complex, indicating that the efficiency of conversion of absorbed light to electrons is constant throughout the spectrum, regardless of whether the incident light is absorbed by the central unit or by the terminal ones. This indicates that, in agreement with what observed in solution, the light absorbed by the peripheral units is efficiently transferred to the central one, where it is used for electron injection.<sup>34</sup> Thus, the  $[\text{Ru}(\text{bpy})_2(\text{CN})_2]_2\text{Ru}(\text{bpy}(\text{COO})_2)_2^{2-}$  trinuclear complex appears to perform indeed as an antenna-sensitizer molecular device on the surface of TiO<sub>2</sub>. A schematic representation of the sequence of processes that take place on the sensitized electrode is shown in Figure 5b.

When the performance of the antenna-sensitizer complex is compared with that of the mononuclear sensitizer, an extension of the spectral response in the 500–600-nm range is observed (Figure 3). This is a useful result which, however, is not related to the use of a trinuclear species as such, as it simply reflects the energy of the  $\text{Ru} \rightarrow \text{bpy}(\text{COO})_2^-$  MLCT band in the two systems (actually, response in the 500–600-nm range has been obtained by Graetzel and co-workers<sup>35</sup> with the mononuclear  $\text{Ru}(\text{bpy}(\text{COO})_2)_2(\text{H}_2\text{O})_2^{2-}$ ). The specific feature of the antenna-sensitizer device is that, in addition to the absorption in the 500–600-nm range by the sensitizer fragment, the high absorption of the antenna fragments in the 400–500-nm range can also be utilized for light harvesting and sensitization.

Finally, it should be stressed that no effort has been made in this work to achieve high absolute photocurrent efficiencies. The aim was to demonstrate the antenna-sensitizer function and to compare mono- and polynuclear complexes on a relative basis. Thus, simple electrodes of low surface area have been used in this work, and correspondingly small photocurrent values have been recorded in the photoelectrochemical experiments. It is easy, however, to imagine the extension of antenna-sensitizer polynuclear complexes to electrodes of very high surface area such as those developed by Graetzel.<sup>8</sup> Hopefully, this could bring about a further gain in the already remarkable conversion efficiencies reached by state-of-the-art regenerative photoelectrochemical cells<sup>6</sup> for solar energy conversion.

## Conclusions

This work shows that it is possible, by suitable selection of molecular components and appropriate synthetic assembly, to arrive at simple molecular devices that couple the functions of a sensitizer (surface binding and photoelectron injection) and an antenna (intramolecular energy transfer from highly absorbing chromophoric groups). The use of antenna-sensitizer molecular devices may constitute a viable strategy to overcome problems of light harvesting efficiency in the spectral sensitization of wide-bandgap semiconductors.

**Acknowledgment.** This work was supported by the Ministero dell'Università e della Ricerca Scientifica e Tecnologica and by the Consiglio Nazionale delle Ricerche (Progetto Finalizzato Chimica Fine II).

(34) In principle, independent photoelectron injection from the various units of the trinuclear complex with constant efficiency would lead to the same result. In practice, such a case is extremely unlikely, because of the much shorter lifetime and less favorable surface binding properties of the peripheral units relative to the central one.

(35) Liska, P.; Vlachopoulos, N.; Nazeeruddin, M. K.; Comte, P.; Graetzel, M. *J. Am. Chem. Soc.* **1988**, *110*, 3686.